Analysis of critical dimension uniformity for step and flash imprint lithography

David P. Mancini[a], Kathleen A. Gehoski[a], William J. Dauksher[a],
Kevin J. Nordquist[a], Douglas J. Resnick[a], Philip Schumaker[b], Ian McMackin[b]
[a]Physical Sciences Research Laboratories, Motorola Labs, Tempe, AZ USA 85284
[b]Molecular Imprints Inc., Austin, TX 78758

ABSTRACT

Step and Flash Imprint Lithography (SFIL) is one of several new nano-imprint techniques being actively developed. While SFIL has been shown to be capable of sub-30 nm resolution, critical dimension (CD) control of imprinted features must be demonstrated if SFIL is to become a viable and production worthy lithography technique. In the current study, a Molecular Imprints Imprio-100 system was used to imprint resolution patterns on 200 mm wafers. A characterization of critical dimension uniformity over the all-quartz template was done and compared to the same features printed on wafers. This analysis was performed for 100, 80, 50, and 30 nm features in three ways: over a single die using 64 sites arrayed across a 21 mm field, from field-to-field for 37 die across a single wafer, and from wafer-to-wafer for six wafers. Results show that CD's transfer from template to wafer with a slight positive bias which is greatest for 50 and 30 nm line sizes. Feature profiles printed for this study were more rounded and sloped than in previous studies. Despite this, the maximum calculated component of process variation from the SFIL process itself was calculated to be only 6 nm (3σ).

KEY WORDS: Step and Flash Imprint Lithography, SFIL, uniformity, template, across-chip linewidth variation (ACLV)

1. Introduction

In the microelectronics industry, advancement in microlithography is one of the primary reasons for the rapid increase in device performance that has occurred in the last three decades. The ability to print ever smaller features in a reliable and cost effective manner has made possible device performance that only decades ago would not have been imagined. The continuation of this trend, so well described by Moore's Law, depends upon continued improvements in this field. Historically, optical lithography has been the technique of choice for production applications. The use of shorter wavelengths of light combined with dramatic improvements in optics and refinements in resist processing have provided the capability of producing features below 100 nm in a production environment. The relationship of these critical parameters is described in the Rayleigh equation (1), where R relates to minimum feature size resolvable, λ is the wavelength of light used for exposure, NA is the numerical aperture of the lens, and k_1 is the proportionality constant which incorporates processing performance. The Rayleigh equation by itself does not foretell an end to this progress provided migration to shorter wavelengths, improvements in processing, and use of higher NA optics continues unabated.

$$(1)\quad R = k_1 \lambda / NA$$

Currently, the industry has recognized 157 nm lithography and Extreme Ultra Violet Lithography (EUVL) as two leading candidate techniques to eventually supplant 193 nm lithography. These Next Generation Lithography (NGL) methods use for irradiation photons having 157 nm and 13.4 nm respective wavelengths. In principle, both techniques offer the promise of improved resolution, and of thereby reserving their place in the progression of optical-based technologies. However, in practice, neither has a clear pathway, since both technologies must overcome significant hurdles before they can be successfully integrated into a fab environment. Historically, progress to the next wavelength node has never been easy, but in the past many of the critical materials issues were to a great extent transferable from the previous node. Arguably, proceeding beyond 193 nm to the next shorter wavelength will be a much more difficult and expensive task than ever before. This is largely due to the poor transparency of most materials to light at short wavelengths (<180 nm). As a result, an entire battery of new

materials technology development must take place in the effort to find suitably performing substitutes. These technical hurdles aside, the cost of ownership (CoO) of either 157 nm or EUV lithography may become the most formidable obstacle of all. CoO studies that have been done for EUVL and 157 nm lithography promise that each will exceed the historical growth rate in lithography tool costs which has been exponential[1].

At the same time, imprinting techniques are also being actively developed as an alternative approach to nanolithography. These techniques are based to a significant degree on contact printing, and offer the possibility of much greater simplicity and lower cost, while producing sub-100 nm resolution. Step and Flash Imprint Lithography (SFIL) is one such technique that holds much promise as an NGL. The process details and mechanics of SFIL have been thoroughly described elsewhere.[4,5,6] SFIL eliminates the need for expensive and complex optics and light sources since it does not depend on the creation and transfer of an aerial image. To form images in SFIL, a low viscosity, photocurable monomer is dispensed in ultra-low volumes at the point of use just prior to imprinting. In this manner, the need for expensive resists and processing tracks is eliminated. Compared to alternative nanoimprint techniques, SFIL uses only low pressures and ambient temperatures to form images. This characteristic by itself offers the potential for improved overlay accuracy as template and substrate distortions are minimized. SFIL has also demonstrated a very high level of resolution and printing repeatability for features down to 30 nm, resolving even small anomalies found on the templates themselves.[2,3] Figure 1 shows an example of a template defect (a field butting error estimated to be less than 5 nm in size) consistently printing onto a wafer.

As with the two leading NGL's, SFIL must overcome its share of technical problems to become a viable and production-worthy lithography method. Issues such as defects, residual layer thickness, template inspection and repair, and overlay accuracy must be solved. In addition, reliable replication of critical dimensions must also be demonstrated. This characteristic, across-chip linewidth variation (ACLV), must be minimal to take full advantage of the resolution capabilities of SFIL. In the current study, an all-quartz template is used to imprint resolution patterns on 200 mm wafers. Critical dimension (CD) uniformity across a single field, across a single wafer, and from wafer-to-wafer for several wafers, is evaluated and statistically analyzed. Linewidths measured on the template are compared to those found on printed wafers, and surface mapping of these data is used to display the results.

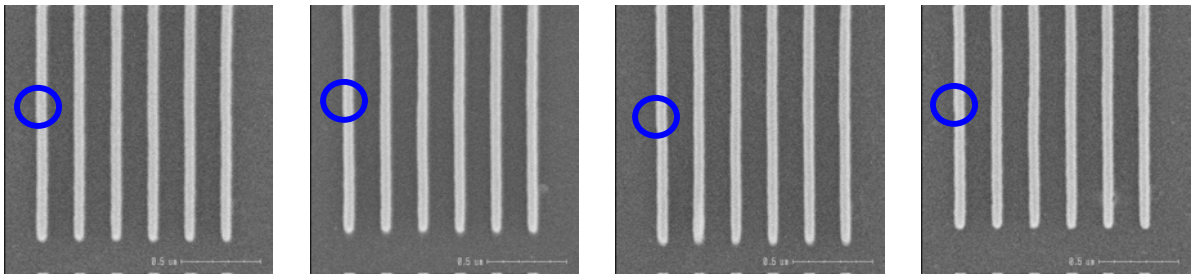

Figure 1. 30 nm lines from four different imprinted die. Circled areas show 2-4 nm stripe butting error, transferred from the template, resolved consistently[2].

2. Experimental

Templates were fabricated on standard 6" × 6" × 0.25" (6025) quartz mask blanks supplied by Ulcoat USA, Inc. Chromium films were deposited onto mask blanks using an MRC 603A sputtering system. Electron beam patterning of templates was done using a Leica VB6 electron beam exposure system with a thermal field emitter source operating at a beam accelerating voltage of 100 keV. The patterns were exposed using a pixel size of 5 nm. All coating and baking operations were done on EV Group model 150/160 coat and bake tracks. ZEP 520A positive e-beam resist supplied by Zeon Chemical was used for defining resolution patterns. All dry etches including etches of resist scum, chromium films, and quartz template relief were done in a Unaxis VLR tool. Template pedestals were defined optically using a 1X contact print mask in conjunction with an OAI 5000 contact aligner. Shipley SPR 220-4.5 positive resist was used to mask the wet buffered oxide (BOE) etch used to form template pedestals. Resist processing for pedestal definition was done on a Laurel spinner, with baking done on a Cee model 1000 hotplate. Chromium films were wet stripped in a bath of ceric ammonium nitrate. Templates were cut from the 6025 blank quartz plate using a diamond saw by American Precision Dicing. Top down SEM images and critical dimension measurements were taken using a Hitachi S-7800 CD SEM. Cross-sectional SEM photos were taken using a Hitachi S4500 SEM. Quartz templates were measured using an accelerating voltage of

3000V and a beam current of 8 μA. Imprinted wafers were measured using 1000V and 4 μA. The working distance for both substrate types was 4 millimeters. Recorded linewidth dimension is the result of an averaging of 32 separate points measured along each line. These points were taken using a 50 % threshold value.

Imprinting was done using an Imprio 100 system manufactured by Molecular Imprints Inc., Austin Texas. All imprinting was done on 200 mm silicon wafers. Prior to imprinting, the wafers were coated with a 600 Å planarizing layer of Brewer Science DUV30J anti-reflective coating (ARC).

3. Results and Discussion

3.1 Template layout and characterization

For ease of manufacture, and economy of both processing time and materials, four individual 25 mm square templates were laid out and fabricated on a single 6025 substrate. The templates were arranged as a 2 × 2 array with a center-to-center spacing of 74.4 mm. The active area of each template was raised to form a pedestal by etching the background (non-printable areas) in a wet buffered oxide etch (BOE) solution. The targeted height of the pedestal measured approximately 15 μm. Individual templates were cut from the 6025 plate by measuring from the pedestal edge 20 mm in each direction. The final template after dicing is a square, 65 mm on a side, with the raised active region centered. Figure 2 shows a diagram of the layout of a 6025 plate before dicing (a), and depicts a single template cut from a plate (b).

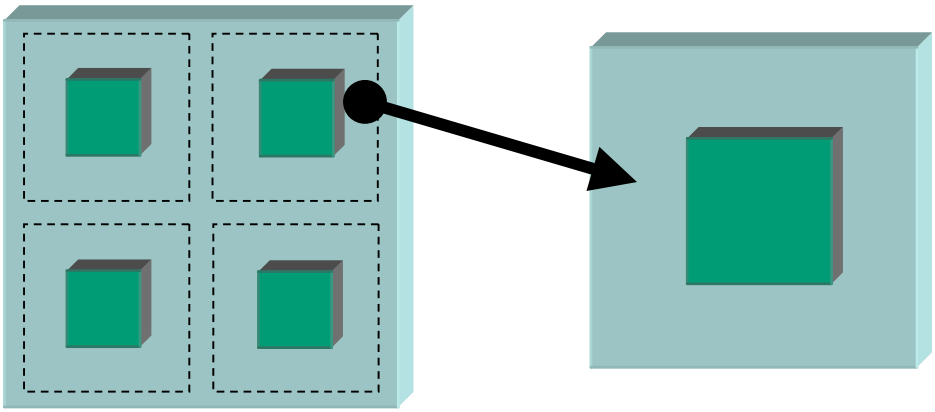

Figure 2. a) 6025 plate with layout of four SFIL pedestal templates. b) single SFIL pedestal template, 65 mm × 65 mm external dimension, with 25 mm square active (center) area.

Measurements of final template CD's were done using a Hitachi S7800 CD SEM. All CD measurements were taken at 200kX magnification, while for image capture, the magnification was adjusted to allow a cluster of dense lines to fit the capture window. Linewidths were measured on the bare quartz surface without benefit of a conductive coating. The resolution pattern used was laid out on each template in a 8 × 8 array, each site spaced 3,000 μm apart so as to cover a square area approximately 21 mm on a side. The layout of the array and the resolution pattern is shown in Figure 3. Line sizes of 100, 80, 50, and 30 nm, both isolated and having 100 nm spaces, were chosen for analysis.

Template CD maps shown in Figure 4 depict linewidth variation as a function of field position for each given line size. This delta is found by taking the difference between the point CD measurement and the overall mean CD calculated from all 64 points in the field. The mean (X) and variation (3σ) of each line size measured on the template is summarized in Table 1. It is clear from this data that there is a nonlinear bias in absolute CD from nominal for all line sizes, starting as positive (> nominal) for 100 nm lines and becoming negative (< nominal) at 30 nm. Not surprisingly, dense lines at each node are larger than their isolated counterparts, the result most likely of e-beam proximity effects at exposure. No discernable regular pattern of CD variation is demonstrated within the field at any line size. Dense line CD's at 100 and 30 nm were particularly uniform as reflected in their small 3σ values of 4.3 and 4.5 nm respectively.

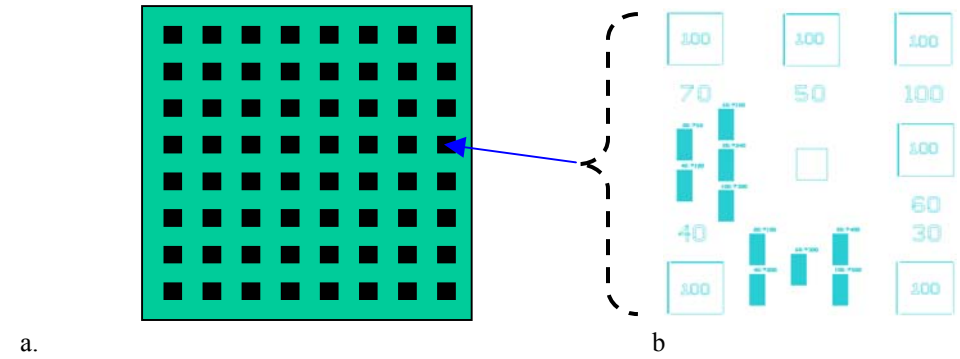

Figure 3. (a) Layout of a single field, (b) Resolution pattern arrayed 8 × 8 in each 25 mm field.

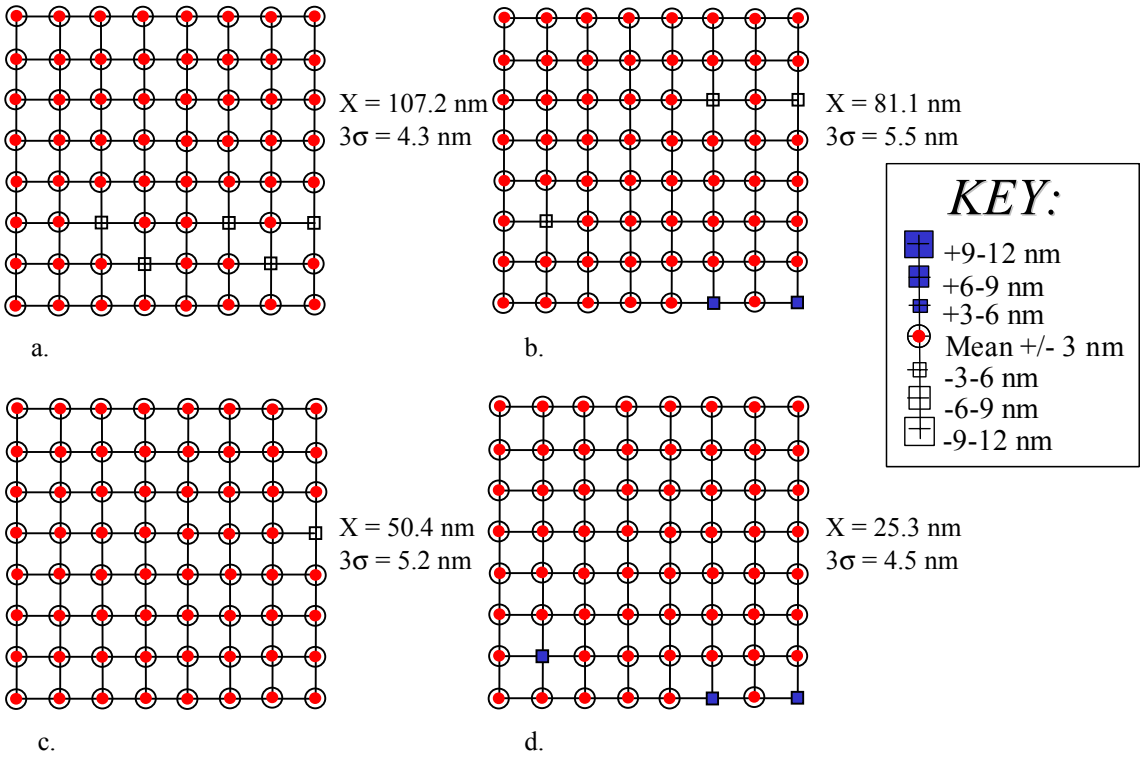

Figure 4. Template critical dimension maps taken over a single template field for 100/100 (a), 80/100 (b), 50/100 (c), and 30/100 nm (d) dense lines.

3.2 Wafer printing results - Across Field Linewidth Variation

A critical dimension map taken from printed wafers across a single field was generated in a manner similar to that used for the template, with all 64 field sites included. This difference between measured CD taken point-by-point, and the overall field mean is plotted in Figure 5 for each line size. Compared to the data shown in Figure 4, this data set shows that features at all CD nodes measured consistently larger than corresponding template features. While the reason for this difference is not known, the cause may simply be due to the difference in the way in which the SEM captured template CD's versus resist CD's. This disparity is observed to increase as feature size decreases. 100 nm dense or isolated lines printed, on average, only 1-2 nm over template CD's, while at the 30 nm node this difference has grown to approximately 11-12 nm. (See Table 1 for isolated line data) Variability also grew compared to the template as reflected by an increase in 3σ values, but grew more at the 100 nm node than for other line sizes. Variation remained constant or increased only slightly at all other CD nodes.

This factor is true even for 30/100 lines which displayed a remarkably tight CD spread. As with the template, no obvious patterns of CD variation are evident.

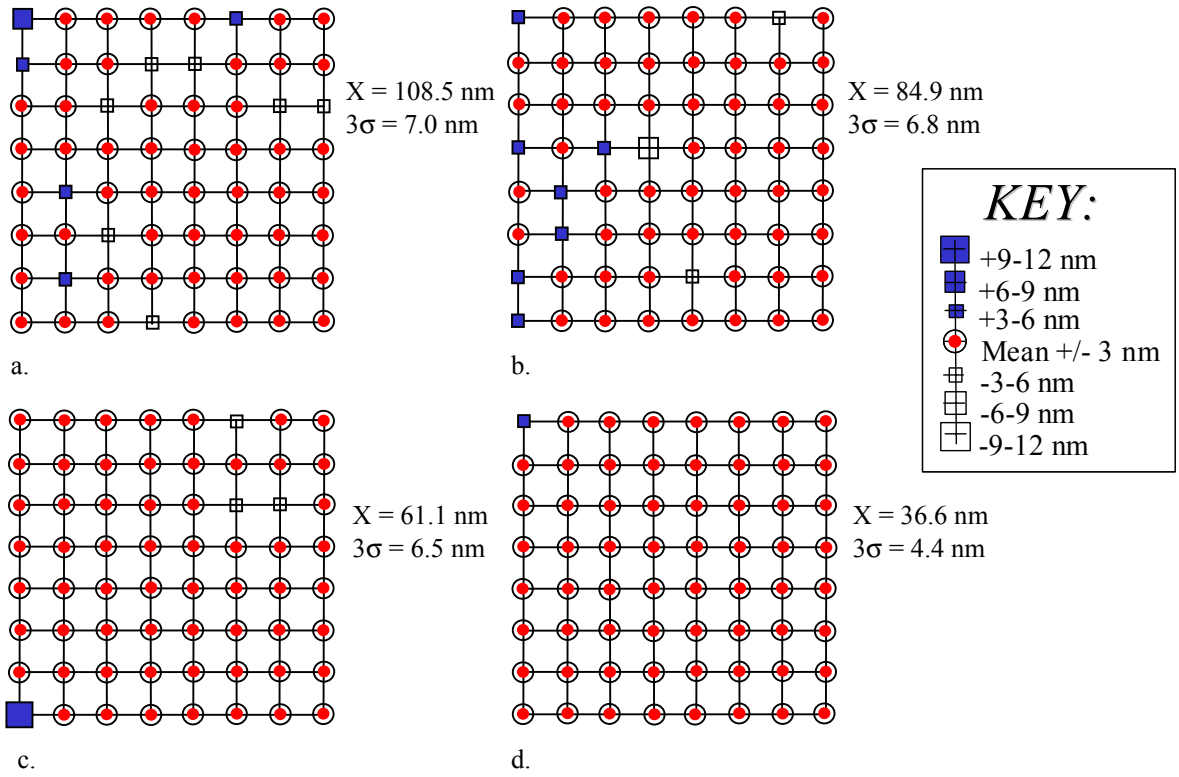

Figure 5. Critical dimension maps taken over a single printed wafer field for 100/100 (a), 80/100 (b), 50/100 (c), and 30/100 nm (d), dense lines.

3.3 Wafer printing results – Across-Wafer CD Uniformity

Field-to-field CD uniformity was evaluated by measuring lines of the same site in each of 37 fields printed across a single wafer. These values are then used to calculate the mean and standard deviation. This data set, mapped in Figure 6, also showed a similar slight to moderate positive CD bias as that shown for a single field. The bias between wafer and template again was negligible at 100 and 80 nm, but became more significant at 50 and 30 nm, increasing to 8-11 nm. In all cases, across-wafer averages were within a few nanometers of the averages for a single field. Variability remained tight and comparable with single field values, with 30/100 lines again showing the smallest value of 3σ = 2.9 nm. Again, there were no apparent patterns of CD variation for any part of the wafer.

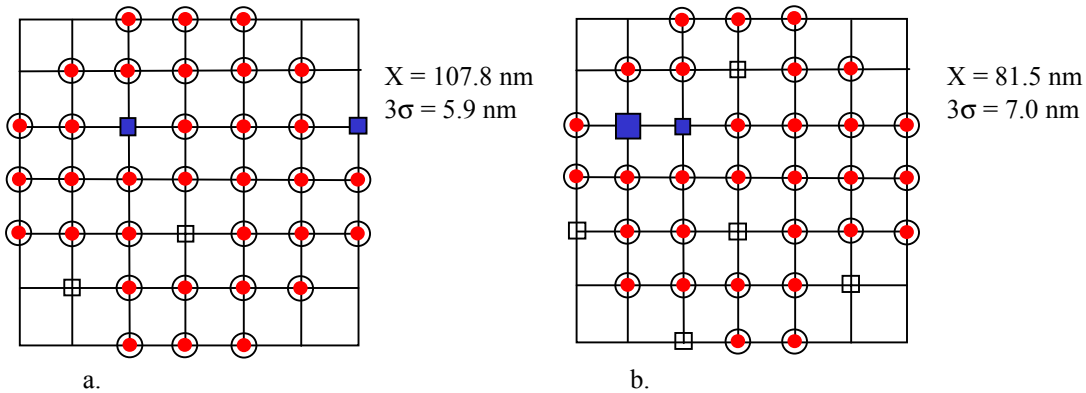

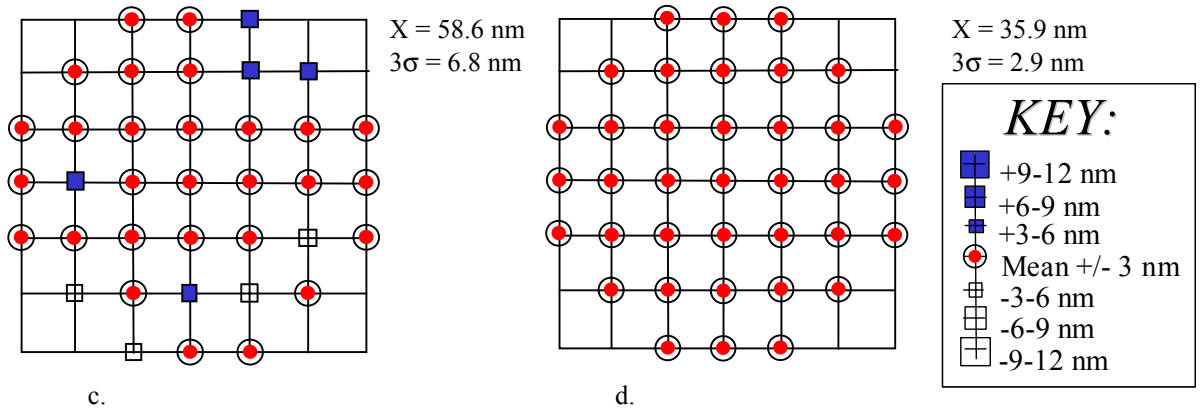

Figure 6. Critical dimension maps taken over all 37 die of a single wafer for 100/100 (a), 80/100 (b), 50/100 (c), and 30/100 nm (d) lines.

3.4 Wafer printing results – Wafer-to-Wafer CD Uniformity

Wafer-to-wafer printing uniformity was also examined using six wafers printed consecutively. Five die on each wafer were chosen, with a single site from each of these die measured for all four CD sizes. The CD's recorded for each line size were averaged to give an overall wafer average. These average values (one per wafer, six for each line size) were then averaged to arrive at a final wafer-to-wafer average for each size node. This data is presented graphically in Figure 7a, and a diagram of the layout of these wafers and the sites chosen is shown in Figure 7b.

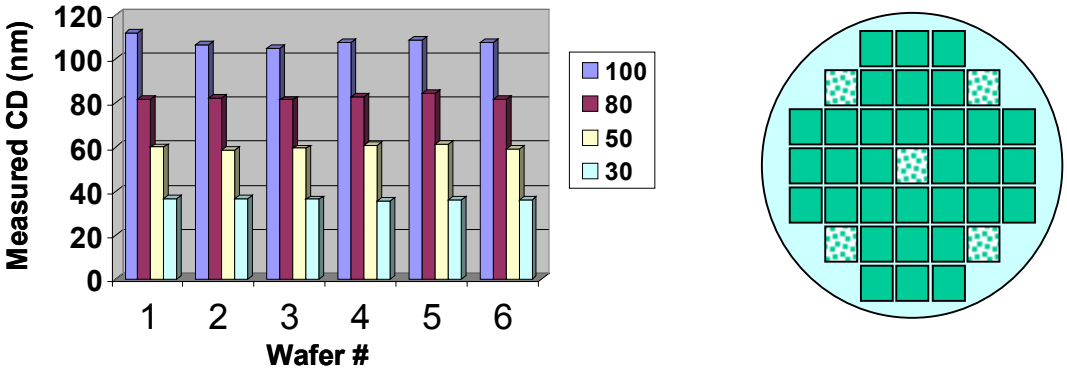

Figure 7. Critical dimension measurements for 100/100, 80/100, 50/100, and 30/100 nm lines taken from a string of consecutively printed wafers (a), diagram of the layout of wafer showing measurement sites (b).

Mean CD for all line sizes was remarkably consistent with all previous tests, varying by less than 3 nm for each set. Variability was also very low, with especially repeatable data recorded at the 30 nm node. Here 3σ values were only 1.5 nm. A summary of all data is shown in Table 1. Isolated line data was recorded only for the template and for the single imprinted field.

Target CD Size (nm)	Template		Across Field (wafer)		Across Wafer		Wafer to Wafer	
	X (nm)	3σ (nm)	X (nm)	3σ (nm)	X (nm)	3σ (nm)	X (nm)	3σ (nm)
100/100	107.2	4.3	108.5	7.0	107.8	5.9	107.9	6.8
100 iso	102.5	6.6	103.4	9.2	N/A	N/A	N/A	N/A
80/100	81.1	5.5	84.9	6.8	81.5	7.0	82.5	3.5
80 iso	68.8	8.7	74.6	8.8	N/A	N/A	N/A	N/A
50/100	50.4	5.2	61.1	6.5	58.6	6.8	59.9	3.0
50 iso	43.6	6.2	53.7	7.1	N/A	N/A	N/A	N/A
30/100	25.3	4.5	36.6	4.4	35.9	2.9	36.1	1.5
30 iso	21.7	5.3	33.5	7.0	N/A	N/A	N/A	N/A

Table 1. Summary of data for template and wafer CD measurements.

3.5 SFIL process variance

It is desirable to estimate the amount of CD variability directly attributable to the SFIL process itself. From the data collected at each CD node, across-field SFIL variation can be estimated by subtracting the component variances of other factors from the total across-field variance, leaving the contribution of the SFIL process as a remainder. The total across-field CD variance can be taken to be the sum of three separate components: variance of the template field, variance of the SEM measurement itself, and variance of the SFIL process. Expressed mathematically:

$$(2) \quad \sigma^2_{AF} = \sigma^2_{T} + \sigma^2_{SEMR} + \sigma^2_{SAF}$$

where: σ^2_{AF} = variance of printed across-wafer data, σ^2_{T} = variance of template data, σ^2_{SEMR} = variance of SEM measurement on resist features, and σ^2_{SAF} = SFIL contribution to across-field CD variance. Solving for, σ^2_{SAF}:

$$(3) \quad \sigma^2_{SAF} = \sigma^2_{AF} - \sigma^2_{T} - \sigma^2_{SEMR}$$

Consideration must be taken of the surface being scanned with a SEM when estimating its variance component. For quartz, this value was found by measuring the same 50 nm site on a template 32 times. The value of variance for this quartz sample was found to be 0.70. Finding this value on SFIL resist features was more difficult due to erosion (line slimming) which occurred as several measurements of the same location were taken. As a result, this value of 3σ = 3.5 nm (or σ^2 = 1.36) was taken from previous resist studies.[2] The variance component of CD's contributed by SFIL taken across a wafer can then be estimated using a similar approach:

$$(4) \quad \sigma^2_{SAW} = \sigma^2_{AW} - \sigma^2_{SEMR}$$

where σ^2_{SAW} = variance of SFIL process across-wafer, and σ^2_{AW} = variance of across-wafer measured data. Here the term for variability of the template field is omitted and assumed to be zero since all measurement sites on wafers arose from the identical template site. This approach was not taken to determine the wafer-to-wafer variance component because of the small data sample size of only six data points (wafers). However, Figure 7a illustrates graphically the consistency of the average CD for each wafer at all linewidth nodes. The results for across-field and across-wafer variance are summarized in Table 2.

	100 nm	80 nm	50 nm	30 nm
σ^2_{SAF}	2.0	0.42	0.40	0.0
$3\sigma_{SAF}$ (nm)	4.2	1.9	1.9	0.0
σ^2_{SAW}	2.5	4.0	3.7	0.0
$3\sigma_{SAW}$ (nm)	4.7	6.0	5.8	0.0

Table 2. Summary of variances of the SFIL process across-field (AF) and across-wafer (AW) along with 3σ value at each CD node.

3.6 SEM images

Figure 8 shows top down SEM images of imprinted wafers at each of the line sizes under consideration. These micrographs reveal a slight, but acceptable degree of line edge roughness. Figure 9 shows cross sectional SEM photos of typical dense lines at 80, 40 and 30 nm nodes all with pitches of 2:1. These features, while demonstrating a very high, sub-40 nm level of resolution, show profiles that are rounded with considerably less feature height than anticipated. Target etch depth of trenches in the template was 100 nm, but it is evident that printed feature height was much less than this, coming in at only 55-60 nm.

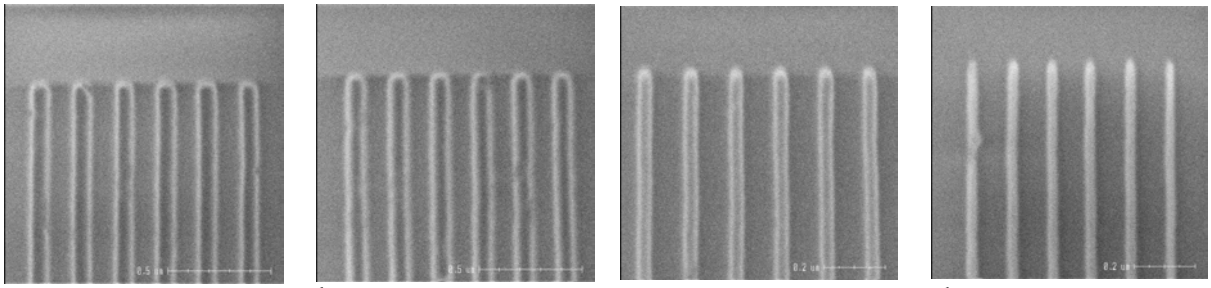

a. b. c. d.

Figure 8. SEM photos from imprinted wafers showing 100/100 (a), 80/100 (b), 50/100 (c), and 30/100 (d) lines.

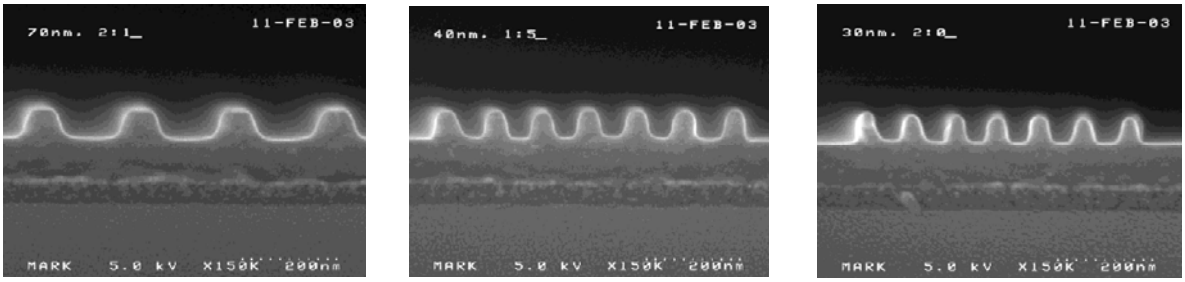

a. b. c.

Figure 9. SEM cross sectional photos from imprinted wafers showing 80 nm (a), 40 nm (b), and 30 nm (c), dense lines all having 2:1 pitch.

The images of Figure 9 of the current study are compared to similarly sized features captured in a previous study shown in Figure 10.[2] Profiles of the latter features, which were generated by a different template, are markedly sharper and more vertical, with less top rounding and less footing. Feature height is also much closer to the 100 nm designed etch depth of the template. In general, replication of the template profile was done with much greater accuracy in these earlier imprints. The reason for the poorer than expected profiles of these recent imprints is not known. It is apparent however, that such a degraded profile will result in an increase of measured linewidth variation. This increase, which cannot be exactly quantified, adds directly to calculated variance component of the

SFIL process. This additional error results in an artificially high degree of expected CD variation from the SFIL process.

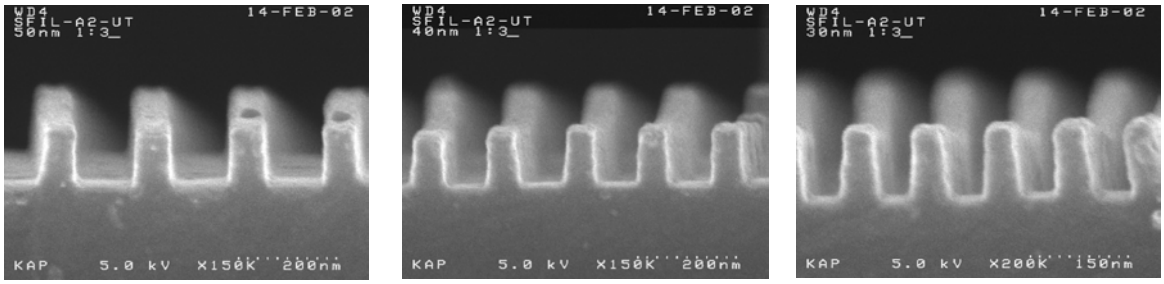

a. b. c.

Figure 10. Cross-section SEM images for 50 nm (a), 40 nm (b), and 30 nm (c) semi-dense lines[2].

4. Conclusions

An analysis of critical dimension variation between an imprinting template and printed wafers has been done for SFIL. This analysis included a characterization and comparison of template CD's with those of printed wafers resulting from the same template. Wafer analysis included CD variability taken across: 64 sites of a single 21 mm field, 37 die printed on a single 200 mm wafer, and selected locations chosen identically from six 200 mm wafers. The results show that the very tight distribution of critical dimensions found on the template was maintained for all wafer prints studied including across field, across a wafer, and from wafer to wafer. The results estimate a maximum of 6 nm 3σ process induced variation for the SFIL process itself. This estimated value is believed however, to be too high since printed features showed an unexpectedly high level of feature rounding accompanied by less than expected feature height. The cause of these poor prints compared to excellent previous results is unknown, but can be assumed to add significantly to the estimated SFIL variance making this estimate of 6 nm 3σ artificially high.

Acknowledgements

The authors gratefully acknowledge Eric Ainley, Adolpho Rios, Jeff Baker, Eric Newlin, Gene Rossi, and David Standfast for their work in processing SFIL templates. The authors also extend their gratitude to Anne Dinsmore, Lester Casoose, Mark Madrid, and Kathy Palmer for providing SEM analysis. Jill Heddleson and Cheryl Jennings are also thanked and acknowledged for their help with statistical analysis. The authors would also like to acknowledge Laura Siragusa for her support in this work.

References

1. S. V. Sreenivasan, C. G. Willson, N. E. Schumaker, and D. J. Resnick, "Cost analysis of step and flash imprint lithography", *Proc. of SPIE*, **vol. 4688**, pp. 903-909, 2002.

2. D. J. Resnick, W. J. Dauksher, D. Mancini, K. J. Nordquist, E. Ainley, K. Gehoski, J. H. Baker, T. C. Bailey, B. J. Choi, S. Johnson, S. V. Sreenivasan, J. G. Ekerdt, C. G. Willson, "High resolution templates for step and flash imprint lithography", *Proc. of SPIE*, **vol. 4688**, pp. 205-213, 2002.

3. W. J. Dauksher, K. J. Nordquist, D. P. Mancini, D. J. Resnick, J. H. Baker, A. E. Hooper, and A. A. Talin, "Characterization of and imprint results using ITO-based step and flash imprint lithography templates", *J. of Vac. Sci. and Technol. B*, **vol. 20**, No. 6, Nov/Dec, pp. 2857-2861, 2002.

4. M. Colburn, A. Grot, M. Amistoso, B. J. Choi, T. Bailey, J. Ekerdt, S.V. Sreenivasan, J. Hollenhorst, C. G. Willson; "Step and flash imprint lithography for sub-100nm patterning", *Proc. of SPIE*, **vol. 3997**, pp. 453-457, (2000).

5. B. J. Choi, S. Johnson, M. Colburn, S.V. Sreenivasan, C. G. Willson; "Design of orientation stages for step and flash imprint lithography", *J. Precision Engineering*, **vol. 25**, no. 3, July 2001.

6. M. Colburn, S. Johnson, M. Stewart, S. Damle, B. J. Choi, T. Bailey, M. Wedlake, T. Michaelson, S.V. Sreenivasan, J. Ekerdt, C.G. Willson; "Step and flash imprint lithography: An alternative approach to high Resolution patterning.", *Proc. of SPIE*, **vol. 3676**, pp. 379-389 (1999).

email address: davidmancini@motorola.com